

Crystal structure of cholesteryl butanoate at 123 K¹

Gye Won Han, B. M. Craven, and David A. Langs*

Department of Crystallography, University of Pittsburgh, PA 15260, and Medical Foundation of Buffalo,*
73 High Street, Buffalo, NY 14203

Abstract Cholesteryl butanoate has a complex crystal structure that differs from those of the three main structure types for cholesteryl esters. It contains four molecules (C₃₁H₅₂O₂) unrelated by crystal symmetry. The molecules are packed in almost planar sheets and have molecular long axes nearly parallel. However, the molecules have different orientations about their long axes and furthermore, in a given sheet, one of the independent molecules is antiparallel to the other three. Viewed down the molecular long axes, each molecule has six nearest neighbors, but the detailed environment is different for the four independent molecules. Thus the molecular arrangement has features that are characteristic of the short-range order present in the cholesteric mesophase. The monotropic transformation from the crystalline to the cholesteric phase occurs at 98°C. The crystal structure has been accurately determined using 12,146 independent X-ray reflections having $\sin\theta/\lambda < 0.63 \text{ \AA}^{-1}$. All hydrogen atoms were located from a difference Fourier and were included in a refinement that gave $R(F^2) = 0.064$. The C-C bond lengths have $\sigma = 0.003 \text{ \AA}$ and C-C-C bond angles have $\sigma = 0.2^\circ$. Conformations for the steroid ring system are similar but there are differences in the C17 side chains and the butanoate chains of the four independent molecules. Analysis of atomic m.s. displacement tensors using a segmented-body model indicates that there are internal librations involving both the C17 and butanoate chains in all molecules.—**Han, G. W., B. M. Craven, and D. A. Langs.** Crystal structure of cholesteryl butanoate at 123 K. *J. Lipid Res.* 1994. 35: 2069–2082.

Supplementary key words complex crystal structure • nematic characteristics • molecular vibrations

The crystal structure determination of cholesteryl butanoate (**Fig. 1**; R = C₃H₇) was undertaken as part of a series involving cholesteryl esters of fatty acids. The longer chain esters containing either saturated (palmitate and stearate) or unsaturated fatty acids (oleate, linoleate) are of great biological importance because of their role in the storage, transport, and metabolism of fats. Crystallographic studies of these and also the shorter chain cholesteryl esters are of interest because they reveal a considerable variety in cholesterol packing arrangements and they illustrate how cholesterol packing is influenced by the presence of fatty acid chains of varying length.

Cholesteryl esters of all saturated and unsaturated fatty acids with chains having six or more carbon atoms that have been studied so far belong to one of three crystal

structure types (1). The hexanoate, heptanoate, and octanoate esters are isostructural, containing so-called monolayers of type II. This structure type is dominated by the close packing of the cholesteryl groups with each other and consequently would appear to be suitable for chains even shorter than C₆. However, the shorter chain esters all feature cholesteryl packing arrangements somewhat different from the monolayers of type II and also different from each other. They include cholesteryl formate (2), chloroformate (3), acetate (4, 5), butanoate (6), isobutanoate (7), and pentanoate (6). From consideration of the cell dimensions reported by Barnard and Lydon (6), it was thought that the crystal structure of cholesteryl butanoate might be similar to that of the acetate ester, except for an increase in the number of molecules in the asymmetric unit from two to four. Thus it was thought that the butanoate structure could be determined by a routine application of the molecular replacement method that has proved to be very successful in almost all structure determinations of cholesteryl esters (1). However, this was not to be. Fourteen years after the initial X-ray data collection at room temperature by Y. Kinoshita and B. M. Craven (unpublished data), the phase problem was eventually solved by probability methods involving the use of a new criterion for testing the reliability of predicted phases (8). Presently we report details of the low temperature data collection, the structure determination, and a description of this unusual crystal structure. We have also used differential scanning calorimetry to observe the phase transformations to the cholesteric and isotropic liquid phases of cholesteryl butanoate. The transition

Abbreviations: m.s., mean square; e.s.d., estimated standard deviation.

¹See NAPS document No. 05138 for 52 pages of supplementary material. This is not a multi-article document. Order from NAPS c/o Microfiche Publications, P.O. Box 3513, Grand Central Station, New York, NY 10162-3513. Remit in advance in U.S. funds only \$17.35 for photocopies or \$1.00 for microfiche. There is a \$15.00 invoicing charge on all orders filled before payment. Outside the U.S. and Canada add postage of \$4.50 for the first 20 pages and \$1.00 for each ten pages of material thereafter, or \$1.75 for the first microfiche and \$0.50 for each fiche thereafter.

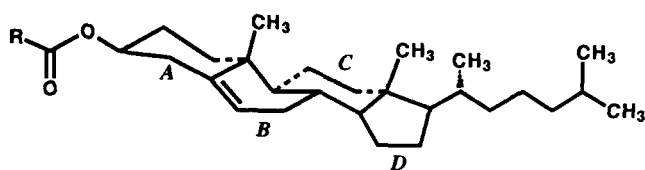


Fig. 1. Chemical structure of cholesteryl esters (R = alkanate or alkenate).

temperatures that we obtained are lower than those (102, 113°C) reported by Gray (9) indicating that our sample for crystallization may not have been as pure as his.

EXPERIMENTAL

Data collection

Cholesteryl butanoate, obtained from Sigma Chemical Co., St. Louis, MO, was recrystallized slowly from a saturated solution in acetone at 0°C. The space group and preliminary cell dimensions, determined from room temperature Weissenberg and precession photographs, agreed with those of Barnard and Lydon (6). An initial set of X-ray diffraction data collected at room temperature by Y. Kinoshita and B. M. Craven (unpublished data) consisted of 3118 reflections having $\sin\theta/\lambda < 0.48 \text{ \AA}^{-1}$. Intensive efforts at structure determination based on these data were unsuccessful. Eventually, a second low temperature (123 K) data set was collected with the aim of measuring many more reflections at higher resolution. Indeed, the number of measured reflections was increased almost fourfold with a corresponding increase in the number of reflection triplets available for use in direct phasing procedures. Furthermore, with reduction in the m.s. amplitudes of the atomic thermal vibrations at lower temperature, it was expected that the structure would be obtainable in much greater detail. The crystal data at the two temperatures are in Table 1(a), a summary of experimental procedures for the 123 K data collection is in Table 1(b), and results of the thermodynamic study are in Table 1(c).

The single crystal was slowly cooled (29 h) to 123 K in a stream of dry nitrogen gas. There was no crystal-to-crystal phase transition. Unit cell dimensions were determined by a least-squares fit to the diffractometer setting angles for 25 reflections with $30 < 2\theta < 50^\circ$. Three monitor reflections, remeasured at 1-h intervals throughout data collection, showed no significant variation. Intensity profiles for all reflections were analyzed and reduced to F^2 -values using the computer programs of Blessing (10). This included application of X-ray absorption corrections (Table 1b).

Structure determination

Unsuccessful attempts were made to solve the phase problem with both the room and low temperature data sets, using molecular replacement (11) and multiple solution direct methods (12) but these yielded, at most, various partial structures in which one or two almost complete independent molecules could be recognized. One series of calculations tested 16,000 random phase sets (13, 14) and failed to produce a solution. Success came with the 123 K data set when the ν -STAT formula (8) was used to identify a reliable starting basis set of 36 restricted phases ($h0l$) definable in terms of seven symbols. The seven symbols were permuted through 16 combinations of phase (0 or π), thereby guaranteeing no more than one wrong symbolic phase (15). Each of the 16 combinations was subject to 10 trials with the RANTAN procedure (14) for the phasing of additional reflections. A solution was

TABLE 1. Experimental data

(a) Crystal data

Cholesteryl butanoate, $C_{31}H_{52}O_2$, $M_r = 456.76$ daltons, monoclinic space group $P2_1$, $Z = 8$ (4 molecules/asymmetric unit)

Kinoshita and Craven ^a	Present results
Room temperature	T = 123 K
$a = 23.65(4) \text{ \AA}$	$a = 22.619(2) \text{ \AA}$
$b = 9.615(7) \text{ \AA}$	$b = 9.553(1) \text{ \AA}$
$c = 25.79(4) \text{ \AA}$	$c = 25.870(2) \text{ \AA}$
$\beta = 94.4(1)^\circ$	$\beta = 94.73(1)^\circ$
$V = 5847(14) \text{ \AA}^3$	$V = 5571(1) \text{ \AA}^3$
$D_x = 1.038 \text{ g cm}^{-3}$	$D_x = 1.089 \text{ g cm}^{-3}$
Mo K_α radiation, graphite monochromator	Cu K_α radiation, Ni-filtered
$\lambda = 0.7093 \text{ \AA}$	$\lambda = 1.5418 \text{ \AA}$
Prismatic colorless crystals exhibiting {101}, {010}, {110}	$0.52 \times 0.36 \times 0.30 \text{ mm}$, elongated on α , mounted with c close to diffractometer ϕ -axis
approx. 0.4 mm	

(b) X-ray data collection (123 K)

Enraf-Nonius CAD-4 diffractometer with low temperature device (liquid nitrogen coolant)
 $\omega/2\theta$ scans; intensity profiles recorded with 96 points/scan;
 maximum speed 2° min^{-1}
 Maximum $\sin\theta/\lambda$: 0.63 \AA^{-1}
 Total number of reflections measured: 16,134
 Number of independent reflections: 12,146
 Internal agreement factor, $R_{int} (F^2) = 0.03$
 Number of reflections with estimated $F^2 < 0$: 207
 Range of X-ray absorption corrections, ($\mu = 5.02 \text{ cm}^{-1}$):
 1.219 to 1.162

(c) Thermodynamic data

Mettler TA-4000 differential scanning calorimeter and Leitz Wetzlar Laborlux 12 Pol polarizing light microscope with Leitz heated stage 350 and temperature controller.

$$\Delta H = 5.32 \text{ Kcal mol}^{-1} \quad \Delta H = 0.16 \text{ Kcal mol}^{-1}$$

98°C 106°C

Crystal \rightarrow Cholesteric mesophase \rightleftharpoons Isotropic liquid

^aUnpublished data.

found for which the E-map revealed most atoms in the tetracyclic rings and some atoms of the butanoate chains. The remaining atoms, including all 208 hydrogen atoms, were located by iterative Fourier methods.

Han (16) describes in more detail the efforts to solve the phase problem for cholesteryl butanoate and also retrospectively compares the initial partial structures obtained by molecular replacement methods with the final correct structure. More recently, cholesteryl butanoate has been used in successful tests of a new phasing procedure based on the minimal function method for partial structure development (17).

Structure refinement

The structure refinements were carried out by a least-squares procedure based on F^2 and included all 12,146 independent reflections (two badly measured reflections were deleted). The residual $\Sigma w(F_o^2 - F_c^2)^2$ was minimized with $w = 1/\sigma^2(F^2)$ and $\sigma^2(F^2) = \sigma_{cs}^2 + (0.02 F^2)^2$ where σ_{cs}^2 is the variance due to counting statistics for each reflection. Because of the large number of variables (2020), consisting of positional parameters for all 340 atoms and m.s. displacement parameters (anisotropic for 132 non-hydrogen atoms, isotropic for 208 hydrogen atoms), refinement was by a block-diagonal procedure with the variables in four large blocks. The variables in the first block were the overall scale factor and all atomic parameters for molecule A. The other blocks each contained the atomic variables for one of the other three independent molecules (B, C, D). The computations were carried out using the POP program (18) with atomic scattering factors from Cromer and Waber (19) for C and O and from Stewart, Davidson, and Simpson (20) for H. The final $R(F^2)$ value of 0.064 was attained with $R_w(F^2) = 0.099$ and goodness-of-fit $S = 1.671$.² The final atomic parameters for C and O are listed in Table 2. Those for H are given by Han (16).

RESULTS AND DISCUSSION

Molecular structure

The molecular structure for molecule A, including the experimentally located hydrogen atoms, is shown in Fig. 2 and the conformations of the molecular framework for the four independent molecules are shown in Fig. 3. Bond distances and angles involving C and O atoms are listed in Table 3(a) and 3(b). Bond torsion angles except those for the steroid ring system are listed in Table 3(c).

² $R(F^2) = \Sigma |F_o^2 - F_c^2| / \Sigma F_o^2$; $R_w(F^2) = \{\Sigma w |F_o^2 - F_c^2|^2 / \Sigma (w F_o^2)^2\}^{1/2}$; $S = \{\Sigma w |F_o^2 - F_c^2|^2 / (m-n)\}^{1/2}$, where m = number of reflections, n = number of parameters.

Within experimental error, bond distances and angles for the crystallographically independent molecules A, B, C, and D are consistent with those found in other accurately determined cholesteryl ester crystal structures (3, 4, 22). The average least-squares estimated standard deviation is 0.003 Å for bond distances and 0.2° for bond angles involving non-hydrogen atoms. The average C-H bond distance in cholesteryl butanoate is 0.99(3) Å and H-C-H angles have an average value of 107(2)°.

The steroid ring systems have a similar conformation in the four independent molecules as indicated by the best least-squares fit (23) for superposition of their C1-C19 fragments. Comparison of molecule A with molecules B, C, and D gave root-mean-square displacements between corresponding atoms of 0.078, 0.077, and 0.124 Å, respectively. Comparison of molecule B with C and D gave 0.054 and 0.106 Å, and C with D gave 0.065 Å. In part, these atomic displacements can be attributed to small but significant differences in the twist of the steroid ring systems about their long axes, as indicated by the differences in the C19-C10-C13-C18 torsion angle (5.5, 9.0, 10.7, and 14.6° for molecules A, B, C, and D, respectively). The conformation of the six-membered B-ring is almost the same in all four molecules; this is also true for the six-membered C-rings. Thus the ring puckering coordinates as defined by Cremer and Pople (24) for the B-rings are in the range $0.47 \text{ \AA} < Q < 0.50 \text{ \AA}$, $50.0^\circ < \theta < 52.4^\circ$ and $206.5^\circ < \phi < 215.5^\circ$, and for the C-rings they are in the range $0.56 \text{ \AA} < Q < 0.57 \text{ \AA}$, $5.3^\circ < \theta < 9.4^\circ$ and $240.2^\circ < \phi < 254.7^\circ$. Greater differences occur in the conformation of the six-membered A-rings ($0.54 \text{ \AA} < Q < 0.55 \text{ \AA}$, $3.8^\circ < \theta < 10.4^\circ$ and $44.2^\circ < \phi < 99.4^\circ$) and in the five-membered D-rings ($0.44 \text{ \AA} < Q < 0.49 \text{ \AA}$ and $180.1^\circ < \phi < 196.8^\circ$). A complete tabulation of puckering coordinates is given by Han (16).

It can be seen from Fig. 3 that the C17 side chain of all four molecules is almost fully extended, as in most cholesteryl ester crystal structures (1). The terminal isopropyl group of molecules A, B, D has a (-)-*gauche* conformation, but that of molecule C has a (+)-*gauche* conformation. The C23-C24-C25-C27 torsion angle is -70.6° for molecule A, -67.1° for molecule B, 63.4° for molecule C, and -62.7° for molecule D. In each molecule the terminal methyl groups C26 and C27 are labeled so that C26 is more nearly *trans* with respect to C23.

The conformation at the ester linkage is similar in molecules A, B, and D, but quite different in molecule C. The torsion angles C2-C3-O3-C28 and C4-C3-O3-C28 at the ester bond have values of 156.8 and -84.0° in molecule A, 148.90 and -91.47° in molecule B, and 159.09 and -79.43° in molecule D, but these values are 84.30 and -155.84° in molecule C.

The butanoate chains are almost fully extended, but in molecule B the alkanoate chain has a conformation not previously observed in cholesteryl ester crystal structures.

TABLE 2. Atomic parameters and their e.s.d.^a

Atom	$x \times 10^5$	$y \times 10^4$	$z \times 10^5$	U_{11}	U_{22}	U_{33}	U_{12}	U_{13}	U_{23}
C1	112891 (8)	384	90672 (8)	202 (8)	206 (9)	261(10)	11 (8)	31 (6)	16 (8)
	25745 (8)	2214(2)	17704 (7)	188 (8)	233(10)	226(10)	25 (8)	15 (6)	2 (8)
	53767 (9)	2155(2)	55761 (7)	258 (8)	208 (9)	209(10)	43 (8)	0 (6)	-10 (8)
	76271 (9)	1775(2)	46865 (7)	249 (8)	274(10)	198(10)	30 (9)	39 (6)	-20 (8)
C2	113560 (8)	637(2)	84900 (8)	234 (8)	220 (9)	259(10)	-1 (8)	52 (6)	30 (8)
	25825 (9)	2155(2)	11787 (7)	223 (8)	259(10)	213(10)	-4 (8)	9 (6)	-2 (8)
	53872 (9)	1703(2)	50087 (8)	263 (8)	275(10)	219(10)	29 (9)	-22 (6)	-14 (8)
	77757 (9)	2028(2)	52658 (8)	301(10)	219(10)	205(10)	21 (8)	55 (9)	-52 (8)
C3	107525 (9)	575(2)	81909 (7)	270 (8)	238(10)	206(10)	-43 (8)	46 (6)	35 (8)
	31918 (9)	2535(2)	10265 (7)	262(10)	270(10)	173 (7)	-17 (8)	22 (6)	-18 (8)
	60118 (9)	1307(2)	48937 (7)	317(10)	173 (9)	177 (7)	8 (8)	20 (6)	-14 (8)
	81391 (9)	827(2)	55090 (7)	307(10)	239(10)	165 (7)	-4 (9)	22 (6)	-46 (8)
C4	103484 (9)	1699(2)	83857 (8)	248 (8)	263(10)	228(10)	4 (8)	1 (6)	26 (8)
	36564 (9)	1538(3)	12738 (7)	245 (8)	319(11)	208(10)	32 (9)	55 (6)	-14 (9)
	62484 (9)	140(2)	52510 (8)	326(10)	189 (9)	206(10)	33 (8)	47 (9)	-6 (8)
	86971 (9)	556(2)	52289 (7)	263 (8)	260(10)	189(10)	23 (8)	0 (6)	-17 (8)
C5	102823 (8)	1526(2)	89618 (7)	214 (8)	190 (8)	229(10)	7 (8)	-5 (6)	6 (8)
	36423 (8)	1496(2)	18612 (7)	217 (8)	195 (9)	216 (7)	22 (8)	49 (6)	-5 (8)
	62103 (8)	519(2)	58172 (7)	279 (8)	133 (8)	196 (7)	16 (7)	54 (6)	7 (6)
	85491 (8)	389(2)	46497 (7)	213 (8)	245(10)	188 (7)	7 (8)	22 (6)	3 (8)
C6	97492 (8)	1490(2)	91384 (8)	218 (8)	189 (9)	235(10)	14 (8)	-18 (6)	15 (8)
	41414 (8)	1654(2)	21661 (7)	207 (8)	209 (9)	251(10)	11 (8)	55 (6)	-6 (8)
	66897 (8)	391(2)	61510 (7)	249 (8)	179 (9)	242(10)	38 (8)	61 (6)	33 (8)
	87389 (9)	-727(2)	44038 (8)	311(10)	242(10)	203(10)	63 (9)	7 (9)	-21 (8)
C7	96317 (8)	1368(2)	97007 (8)	154 (8)	306(11)	261(10)	10 (8)	18 (6)	17 (8)
	41808 (8)	1600(2)	27502 (7)	197 (8)	194 (9)	243(10)	2 (8)	13 (6)	-1 (8)
	67005 (8)	677(2)	67222 (7)	228 (8)	188 (9)	217(10)	29 (8)	18 (6)	13 (8)
	86458(10)	-957(2)	38264 (8)	353(10)	249(10)	211(10)	99 (9)	24 (9)	-4 (8)
C8	101919 (8)	1594(2)	100675 (7)	180 (8)	189 (9)	240(10)	7 (7)	22 (6)	29 (8)
	36203 (8)	1030(2)	29656 (7)	185 (8)	129 (8)	228 (7)	4 (7)	7 (6)	-17 (6)
	60782 (8)	802(2)	69074 (7)	213 (8)	125 (8)	200 (7)	0 (7)	23 (6)	15 (6)
	84521 (8)	382(2)	35369 (7)	233 (8)	191 (9)	183 (7)	21 (8)	35 (6)	-8 (8)
C9	107199 (8)	825(2)	98497 (7)	180 (8)	157 (9)	249(10)	2 (7)	3 (6)	2 (8)
	30637 (8)	1621(2)	26550 (7)	189 (8)	163 (8)	212 (7)	10 (7)	13 (6)	-27 (8)
	56825 (8)	1698(2)	65232 (7)	199 (8)	158 (8)	193 (7)	-5 (7)	20 (6)	-6 (6)
	79585 (8)	1108(2)	38174 (7)	219 (8)	211 (9)	177 (7)	30 (8)	32 (6)	-36 (8)
C10	108599 (8)	1411(2)	93152 (7)	176 (8)	171 (9)	251(10)	-8 (7)	19 (6)	22 (8)
	30376 (8)	1246(2)	20691 (7)	176 (8)	193 (9)	201 (7)	11 (7)	23 (6)	-30 (8)
	56090 (8)	1033(2)	59751 (7)	233 (8)	150 (8)	194 (7)	-20 (7)	25 (6)	-1 (6)
	81790 (8)	1544(2)	43793 (7)	233 (8)	192 (9)	175 (7)	9 (8)	29 (6)	-9 (8)
C11	112672 (8)	745(2)	102467 (8)	170 (8)	282(10)	254(10)	8 (8)	25 (6)	31 (8)
	24941 (8)	1234(2)	29128 (7)	187 (8)	230(10)	204 (7)	8 (7)	18 (6)	-26 (8)
	50845 (8)	2069(2)	67385 (7)	203 (8)	247(10)	213(10)	33 (8)	6 (6)	-13 (8)
	76705 (8)	2346(2)	35055 (8)	271(10)	230(10)	215(10)	65 (8)	37 (9)	-11 (8)
C12	111261 (8)	235(2)	107851 (8)	173 (8)	213 (9)	253(10)	26 (8)	9 (6)	16 (8)
	25152 (8)	1622(2)	34915 (7)	201 (8)	222 (9)	212(10)	32 (8)	26 (6)	-11 (8)
	51464 (8)	2657(2)	72939 (7)	235 (8)	187 (9)	201(10)	35 (8)	30 (6)	-6 (8)
	74904 (9)	1998(2)	29329 (7)	237 (8)	262(10)	201(10)	56 (8)	31 (6)	7 (8)
C13	106404 (8)	1127(2)	110049 (7)	181 (8)	175 (8)	235(10)	18 (7)	19 (6)	6 (8)
	30516 (8)	939(2)	37979 (7)	198 (8)	147 (8)	216 (7)	-3 (7)	25 (6)	-5 (6)
	55012 (8)	1669(2)	76702 (7)	207 (8)	166 (8)	177 (7)	-11 (7)	32 (6)	0 (6)
	80143 (8)	1403(2)	26627 (7)	224 (8)	191 (9)	178 (7)	14 (8)	22 (6)	3 (8)
C14	100946 (8)	1050(2)	106065 (7)	163 (8)	196 (9)	257(10)	11 (7)	12 (6)	7 (8)
	36064 (8)	1425(2)	35366 (7)	196 (8)	145 (8)	216 (7)	-7 (7)	19 (6)	-17 (6)
	61060 (8)	1451(2)	74471 (7)	210 (8)	160 (8)	190 (7)	-10 (7)	24 (6)	16 (6)
	82229 (8)	90(2)	29749 (7)	228 (8)	181 (8)	171 (7)	29 (7)	41 (6)	-17 (6)
C15	95966 (9)	1720(3)	108929 (8)	207 (8)	331(12)	284(10)	74 (9)	36 (9)	25 (9)
	41288 (8)	964(2)	39145 (7)	213 (8)	174 (9)	244(10)	2 (8)	3 (6)	-19 (8)
	64914 (9)	734(2)	78857 (7)	227 (8)	272(10)	215(10)	37 (8)	11 (6)	41 (8)
	86267(10)	-671(2)	26205 (8)	304(10)	253(10)	198(10)	90 (9)	45 (9)	-14 (8)
C16	97676 (9)	1403(3)	114725 (8)	218 (8)	353(12)	269(10)	76 (9)	59 (9)	25 (9)
	38851 (8)	1146(2)	44564 (7)	224 (8)	209 (9)	234(10)	3 (8)	-6 (6)	12 (8)
	62816 (9)	1416(2)	83798 (7)	251 (8)	300(11)	197(10)	23 (9)	9 (6)	17 (8)
	83249 (9)	-406(2)	20688 (7)	331(10)	231(10)	175 (7)	67 (9)	42 (9)	8 (8)
C17	103579 (8)	567(2)	114905 (7)	196 (8)	211 (9)	236(10)	16 (8)	22 (6)	5 (8)
	32101 (8)	1484(2)	43613 (7)	217 (8)	159 (8)	221 (7)	-10(7)	4 (6)	11 (8)
	57111 (8)	2285(2)	82116 (7)	215 (8)	214 (9)	192 (7)	-11(8)	27 (6)	-14 (8)
	78518 (8)	765(2)	21134 (7)	250 (8)	214 (9)	162 (7)	10 (8)	12 (6)	0 (8)

TABLE 2. Continued

Atom	$x \times 10^5$	$y \times 10^4$	$z \times 10^5$	U_{11}	U_{22}	U_{33}	U_{12}	U_{13}	U_{23}
C18	108630(10)	2641(2)	110932 (9)	280(10)	198(10)	302(10)	- 21 (8)	- 7 (9)	- 13 (8)
	29826 (9)	- 665(2)	37993 (8)	255(10)	169 (9)	248(10)	- 9 (8)	27 (9)	- 2 (8)
	51700 (9)	282(2)	77349 (8)	289(10)	208 (9)	232(10)	- 45 (8)	48 (9)	- 16 (8)
	85157 (9)	2491(2)	26402 (8)	279(10)	235(10)	228(10)	- 33 (8)	20 (9)	3 (8)
C19	111488 (9)	2877(2)	93599 (8)	241 (8)	190 (9)	300(10)	- 27 (8)	30 (9)	2 (8)
	28635 (9)	- 298(2)	19714 (8)	246(10)	195 (9)	271(10)	- 13 (8)	4 (9)	- 36 (8)
	51773(10)	- 213(2)	59561 (8)	317(10)	232(10)	276(10)	- 99 (9)	43 (9)	- 57 (9)
	85511(10)	2899(2)	43842 (8)	330(10)	239(10)	237(10)	- 48 (9)	30 (9)	- 22 (8)
C20	107334 (9)	586(2)	120183 (8)	226 (8)	244(10)	257(10)	9 (8)	30 (6)	8 (8)
	28591 (9)	962(2)	48118 (7)	269 (8)	211 (9)	207(10)	- 5 (8)	19 (6)	5 (8)
	52799 (9)	2310(2)	86436 (7)	244 (8)	269(10)	203(10)	- 22 (8)	41 (6)	- 15 (8)
	78040 (9)	1769(2)	16467 (7)	278 (8)	242(10)	170 (7)	23 (8)	28 (6)	21 (8)
C21	111434(10)	- 693(3)	120616 (9)	272(10)	373(13)	289(10)	96(10)	10 (9)	- 1 (9)
	21891 (9)	1195(3)	47105 (9)	275(10)	328(12)	272(10)	- 10 (9)	47 (9)	17 (9)
	46950(10)	3063(3)	84809 (9)	264(10)	428(13)	248(10)	42(10)	31 (9)	- 35(10)
	73394(10)	2922(3)	16975 (8)	363(10)	304(11)	234(10)	97(10)	25 (9)	49 (9)
C22	103486 (9)	610(3)	124795 (8)	261(10)	412(13)	237(10)	67(10)	15 (9)	- 3 (9)
	30933(10)	1675(3)	53232 (8)	368(10)	260(11)	219(10)	- 83 (9)	31 (9)	- 16 (9)
	55831(10)	2998(3)	91321 (8)	294(10)	335(12)	202(10)	- 70 (9)	60 (9)	- 33 (9)
	76724(10)	981(3)	11327 (7)	350(10)	273(10)	188(10)	- 17 (9)	- 2 (9)	22 (8)
C23	106957(10)	610(3)	130125 (8)	287(10)	379(13)	245(10)	42(10)	10 (9)	29 (9)
	28865(10)	1025(3)	58151 (8)	333(10)	281(11)	239(10)	- 32 (9)	21 (9)	4 (9)
	53082(10)	2695(3)	96378 (8)	323(10)	402(13)	199(10)	- 82(10)	47 (9)	6 (9)
	77344(10)	1891(2)	6517 (7)	392(10)	259(10)	170(10)	6 (9)	3 (9)	3 (8)
C24	103102(10)	1000(3)	134469 (8)	314(10)	384(13)	237(10)	81(10)	7 (9)	22 (9)
	31619(11)	1699(3)	63099 (9)	398(13)	451(14)	253(10)	- 159(11)	48 (9)	- 30(10)
	56459(10)	3395(3)	101005 (8)	310(10)	377(13)	220(10)	- 15 (9)	42 (9)	- 35 (9)
	77302(10)	1093(3)	1452 (8)	397(10)	259(10)	206(10)	- 5 (9)	4 (9)	- 2 (9)
C25	106290(10)	918(3)	139919 (8)	301(10)	355(12)	218(10)	- 12 (9)	- 6 (9)	71 (9)
	30299(10)	963(3)	68143 (8)	318(10)	480(14)	223(10)	- 14(11)	15 (9)	7(10)
	54091(11)	3146(3)	106275 (9)	322(10)	546(15)	215(10)	- 5(11)	44 (9)	- 15(10)
	78717(9)	1993(2)	- 3184 (7)	257 (8)	316(11)	197(10)	1 (9)	15 (6)	5 (8)
C26	102781(14)	1673(4)	143856(10)	547(15)	575(18)	258(10)	104(14)	5(12)	12(11)
	34122(16)	1540(7)	72765(12)	531(18)	1342(44)	273(14)	- 309(24)	- 30(12)	- 90(20)
	57363(13)	4058(3)	110416(10)	491(15)	543(17)	247(10)	131(13)	- 10 (9)	- 98(11)
	79337(13)	1100(3)	- 7988 (9)	513(15)	472(15)	228(10)	45(13)	57 (9)	- 33(10)
C27	107561(16)	- 584(3)	141590(12)	647(18)	405(16)	446(14)	- 5(14)	- 101(15)	144(13)
	23822(10)	1059(3)	69174 (9)	371(10)	259(11)	324(10)	16 (9)	74 (9)	30 (9)
	54368(24)	1632(4)	107902(13)	1259(36)	553(20)	339(17)	- 175(23)	43(18)	69(14)
	74116(10)	3137(3)	- 4342 (9)	349(10)	374(13)	268(10)	39(10)	- 10 (9)	51(10)
C28	104240(9)	358(3)	72959 (8)	295(10)	320(11)	251(10)	- 41 (9)	28 (9)	14 (9)
	35276 (9)	3252(3)	2130 (8)	228 (8)	341(11)	248(10)	- 23 (9)	38 (6)	13 (9)
	60309 (8)	1733(2)	39823 (8)	234 (8)	258(10)	225(10)	32 (8)	30 (6)	42 (8)
	84411 (9)	199(2)	63896 (8)	293(10)	250(10)	234(10)	- 47 (8)	55 (9)	11 (8)
C29	105488(12)	840(3)	67578 (9)	377(13)	608(18)	267(10)	- 158(13)	9 (9)	89(11)
	35059(10)	2938(3)	- 3603 (8)	312(10)	435(13)	236(10)	- 71(10)	41 (9)	1(10)
	59682(10)	1041(3)	34598 (8)	341(10)	334(11)	203(10)	16(10)	42 (9)	19 (9)
	85455(10)	777(3)	69307 (8)	415(10)	278(11)	198(10)	- 62(10)	11 (9)	12 (9)
C30	102281(15)	74(4)	63296(10)	553(18)	761(23)	289(14)	- 250(18)	37(12)	- 15(14)
	29634(11)	2211(3)	- 6086 (9)	327(10)	595(17)	284(10)	- 127(12)	60 (9)	- 83(11)
	58823(10)	2069(3)	30102 (8)	254(10)	403(13)	236(10)	- 10(10)	26 (9)	48 (9)
	84125(11)	- 269(3)	73459 (8)	396(10)	292(11)	210(10)	- 54(10)	- 1 (9)	22 (9)
C31	103410(12)	684(3)	57968 (9)	407(13)	496(16)	265(10)	- 63(12)	40 (9)	11(11)
	29893(12)	2018(3)	- 11900 (9)	367(13)	501(15)	285(10)	4(11)	- 13 (9)	- 61(11)
	58332(11)	1347(3)	24870 (9)	319(10)	634(18)	231(10)	- 42(12)	14 (9)	20(11)
	84980(12)	338(3)	78860 (9)	510(13)	360(13)	211(10)	- 96(11)	- 3 (9)	18 (9)
O3	108429 (6)	843(2)	76487 (5)	300 (8)	309 (8)	202 (7)	- 62 (7)	36 (6)	24 (6)
	31768 (6)	2395(2)	4620 (5)	289 (8)	321 (8)	182 (7)	- 55 (7)	28 (6)	- 9 (6)
	60072 (6)	776(2)	43671 (5)	370 (8)	217 (7)	172 (7)	16 (7)	34 (6)	2 (5)
	82894 (7)	1233(2)	60461 (5)	382 (8)	233 (7)	152 (7)	- 3 (7)	22 (6)	- 13 (5)
O28	100030 (8)	- 318(2)	73971 (6)	398 (8)	603 (12)	265 (7)	- 224 (9)	27 (6)	10 (8)
	38358 (8)	4146(2)	4236 (6)	460(10)	502(11)	311 (7)	- 228 (9)	79 (6)	- 54 (8)
	60946 (7)	2969(2)	40602 (6)	430 (8)	256 (8)	268 (7)	10 (7)	40 (6)	36 (6)
	84767 (8)	- 1008(2)	62716 (6)	450 (8)	234 (8)	284 (7)	- 26 (7)	7 (6)	- 4 (6)

For each atom, parameters on successive lines are for molecules A, B, C, and D. E.s.d.s (in parentheses) refer to the least significant digit. Atomic m.s. anisotropic displacement parameters (units $\text{\AA}^2 \times 10^4$) are defined by the expression: $T = \exp[-4\pi^2 \sum_i \sum_j h_i a_i^ a_j^* U_{ij}]$.

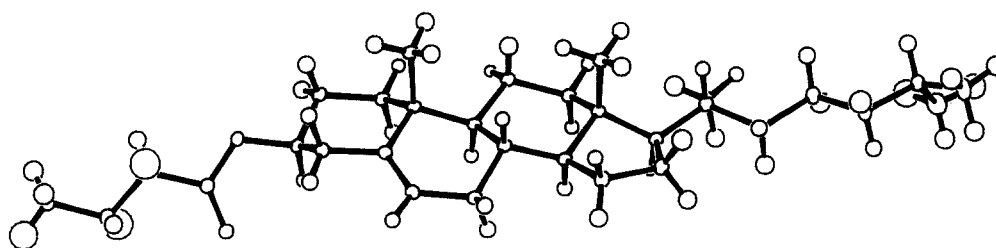


Fig. 2. Molecular structure for molecule A, including the hydrogen atoms which were all located experimentally. Atoms and their m.s. amplitudes of thermal vibration are plotted according to Johnson (21). Thermal ellipsoids (for C and O) or spheres (for H) have 25% probability of enclosing the vibrating atom.

Thus the butanoate chain extends almost *trans* to the carbonyl oxygen O28 rather than to the ester oxygen O3 (Fig. 3). The torsion angle O3-C28-C29-C30 has values 163.6, 169.9, and 151.1° in molecules A, C, and D, respectively, and 23.9° in molecule B.

Molecular thermal vibrations

At 123 K, thermal vibrations for the C and O atoms have root-mean-square amplitudes that range from 0.12 to 0.19 Å in the steroid ring system and from 0.13 to 0.37 Å for the C17 side chains and for the butanoate chains. It must be remembered that the m.s. displacements of the atoms are the sum of contributions from static displacement as well as thermal vibrations. However, in cholesteryl butanoate none of the observed displacements is suspiciously large, and we have no reason to suppose that there is conformational disorder in the structure. The analysis of m.s. atomic displacements was carried out assuming these represent only the thermal vibrations.

The analysis of the thermal vibrations in the crystal began by a least squares fit of mean square (m.s.) displacement parameters (U_{ij} in Table 2) for the C and O atoms, with the assumption that each molecule is vibrating as a rigid body (25).³ For molecules A, B, and C, a moderately good fit was obtained ($R_w = 0.179, 0.219$ and 0.184 , respectively), with a better fit for molecule D ($R_w = 0.126$).

Strong indications of non-rigid behavior were obtained from the observed values of $\Delta = \langle u_m^2 \rangle - \langle u_n^2 \rangle$ which is the difference in m.s. displacement of atoms m and n along the direction of their interatomic separation. The value $\Delta = 0$ should be obtained if atoms m and n are vibrating rigidly together (26, 27). Values $\Delta = 0$ within

experimental error were obtained in all covalently bonded atom pairs, except possibly for C30-C31 in molecule A ($\Delta = 0.0053 \text{ \AA}^2$; 2.6σ) and C28-O3 in molecule D ($\Delta = 0.0037 \text{ \AA}^2$; 2.9σ). However, highly significant non-zero values ($\Delta > 6\sigma$) were obtained for each molecule for atom pairs in which one atom m belongs to the steroid ring system while the other n belongs either to the C17 tail or the butanoate chain. The most significantly non-rigid atom pairs in each category are C17...C27 in molecule A ($\Delta = 0.0154 \text{ \AA}^2$; 9σ) and C6...O28 in molecule B ($\Delta = 0.0167 \text{ \AA}^2$; 13σ).

The analysis continued assuming each molecule to be vibrating as a segmented rigid body. Thus the molecule has overall rigid-body motion as well as internal torsional librations about selected covalent bonds. The procedure used was that of He and Craven (28) with computations using the program EKRT (29). For each internal torsion, the molecule consists of two rigid segments that are in relative motion. The atomic displacements must satisfy the conditions of Eckart (30) that effectively require that the total angular and linear momentum of the molecule about its center remain zero throughout the vibration. All atoms move, including those lying on the torsion axis. Individual internal vibrations are assumed not to interact with each other so that their atomic m.s. displacements are additive.

For the cholesteryl butanoate molecules, the hydrogen atoms were neglected except in calculating the molecular moments of inertia (Table 4). For this purpose, carbon atom masses were augmented by the mass of any covalently bonded hydrogen. Various models were tested by trial and error. All consisted of a rigid steroid ring system together with internal torsions involving the C17 tail and the butanoate group. Little progress was made until a physical coupling was introduced between each internal vibration and the overall rigid body vibrations. Dunitz, Schomaker, and Trueblood (31) have pointed out that when this is done, the m.s. amplitude of the internal torsional vibration $\langle \phi^2 \rangle$ is no longer an independent variable. In principle, only the six terms $\langle \phi l_i \rangle$ and $\langle \phi l_j \rangle$

³In this analysis, $R_w = \{\sum w \Delta^2 / (\sum (w U_{obs}^2))\}^{1/2}$, and $S = \{\sum w \Delta^2 / (m-n)\}^{1/2}$, where $\Delta = U_{obs} - U_{calc}$, $w = \sigma^{-2}(U)$, m = number of observations, and n = number of variables. The sum is over the six U_{ij} components and includes all C and O atoms in the molecule.

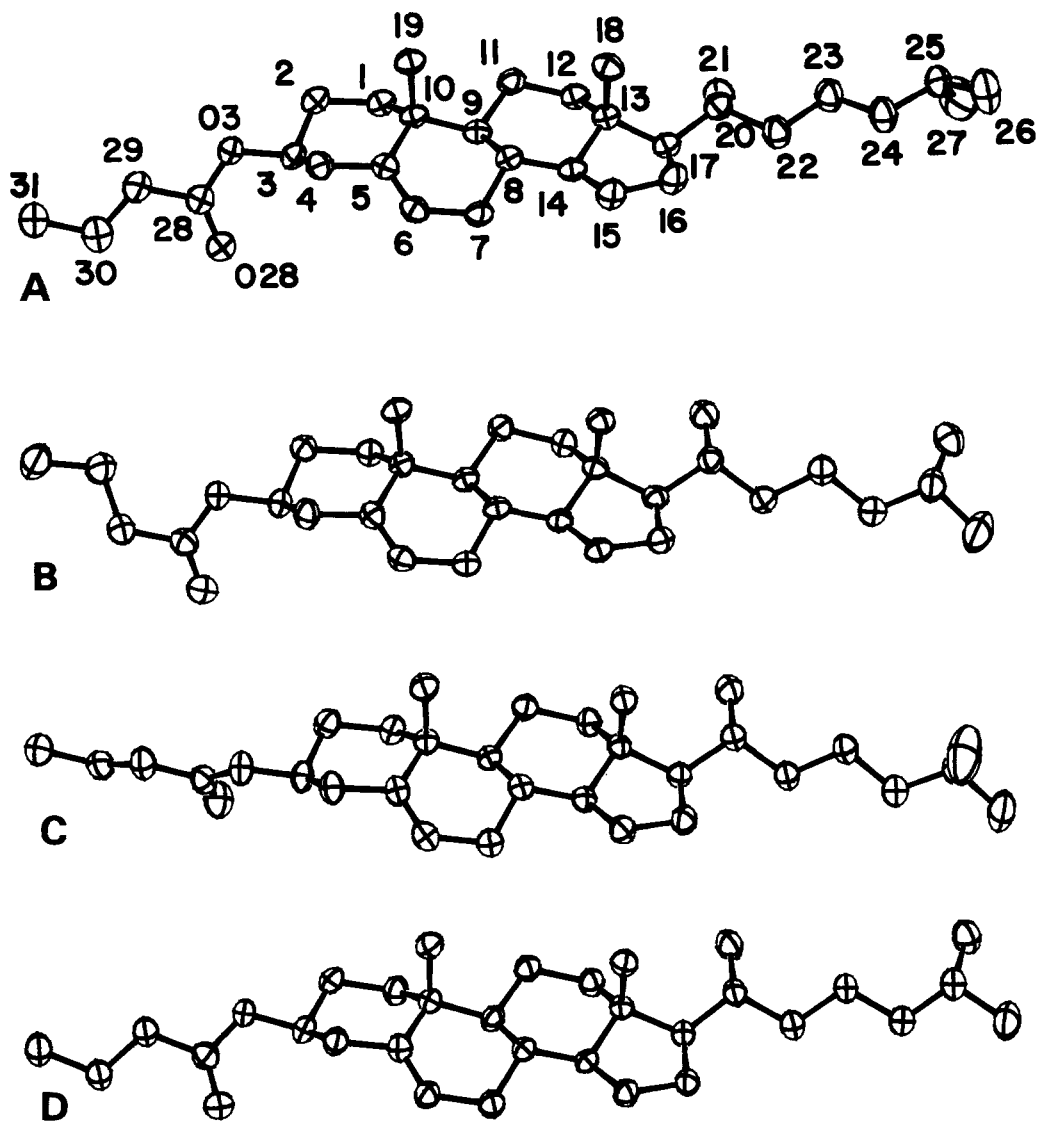


Fig. 3. Molecular structures (hydrogen atoms omitted) for the four independent molecules (A at top through D at bottom). Atom numbering is shown for molecule A. All molecules are shown with the steroid ring system in the same orientation. Atoms and their m.s. amplitudes of thermal vibration are plotted according to Johnson (21). Thermal ellipsoids have 75% probability of enclosing the vibrating atom.

can be determined, where ϕ is the amplitude of an internal vibration and t_j and l_j are Cartesian components of the amplitude of the overall rigid body translation and libration. In the case of a rod-shaped molecule such as cholesteryl butanoate, where it is difficult to distinguish librational motion about the molecular long axes from translational motion perpendicular to this axis, and when internal axes are introduced which are close to the molecular long axes, we expected and found some very strong correlations (>0.98) between variables in the least

squares fitting. These correlations were avoided by omitting all coupling terms between the internal vibrations and the overall rigid body translation, with the exception of $\langle \phi_1 t_j \rangle$ for molecule A (see caption, **Table 5**). The largest remaining least squares correlations (0.94) then involved $\langle \phi_1 t_j \rangle$ in molecule A and the correlation of T_{11} with L_{11} (0.70) for the other molecules. The segmented body models described in **Table 5** give improved agreement over the rigid body model for all molecules, but especially A, B, and C.

TABLE 3. Interatomic distances (Å) and angles (°) with e.s.d.^a

(a) Bond lengths				
Atoms	A	B	C	D
C1-C2	1.532(3)	1.533(3)	1.532(3)	1.528(3)
C1-C10	1.555(3)	1.554(3)	1.549(3)	1.550(3)
C2-C3	1.514(3)	1.508(3)	1.515(3)	1.517(3)
C3-O3	1.457(2)	1.464(2)	1.453(2)	1.456(2)
C3-C4	1.523(3)	1.520(3)	1.517(3)	1.528(3)
C4-C5	1.519(3)	1.523(3)	1.518(3)	1.517(3)
C5=C6	1.325(3)	1.332(3)	1.335(3)	1.331(3)
C5-C10	1.536(3)	1.529(3)	1.533(3)	1.520(3)
C6-C7	1.505(3)	1.507(3)	1.501(3)	1.508(3)
C7-C8	1.535(3)	1.527(3)	1.528(3)	1.529(3)
C8-C9	1.547(3)	1.544(3)	1.541(3)	1.545(3)
C8-C14	1.521(3)	1.527(3)	1.524(3)	1.529(3)
C9-C10	1.548(3)	1.554(3)	1.550(3)	1.554(3)
C9-C11	1.544(3)	1.543(3)	1.546(3)	1.545(3)
C11-C12	1.534(3)	1.539(3)	1.538(3)	1.540(3)
C12-C13	1.536(3)	1.539(3)	1.534(3)	1.534(3)
C13-C14	1.544(3)	1.545(3)	1.542(3)	1.544(3)
C13-C17	1.551(3)	1.561(3)	1.557(3)	1.562(3)
C13-C18	1.541(3)	1.541(3)	1.538(3)	1.543(3)
C14-C15	1.537(3)	1.535(3)	1.534(3)	1.530(3)
C15-C16	1.547(3)	1.558(3)	1.544(3)	1.551(3)
C16-C17	1.553(3)	1.560(3)	1.566(3)	1.560(3)
C17-C20	1.548(3)	1.546(3)	1.543(3)	1.539(3)
C20-C21	1.533(3)	1.533(3)	1.534(3)	1.535(3)
C20-C22	1.534(3)	1.543(3)	1.535(3)	1.536(3)
C22-C23	1.530(3)	1.524(3)	1.522(3)	1.534(3)
C23-C24	1.524(3)	1.520(3)	1.521(3)	1.515(3)
C24-C25	1.532(3)	1.533(4)	1.524(4)	1.531(3)
C25-C26	1.523(4)	1.520(5)	1.524(4)	1.523(3)
C25-C27	1.520(4)	1.513(3)	1.506(5)	1.522(3)
O3-C28	1.343(3)	1.341(3)	1.356(2)	1.354(3)
C28=O28	1.198(3)	1.204(3)	1.204(3)	1.198(3)
C28-C29	1.515(4)	1.510(3)	1.501(3)	1.505(3)
C29-C30	1.469(4)	1.507(4)	1.522(3)	1.516(3)
C30-C31	1.537(4)	1.521(4)	1.515(4)	1.511(3)
(b) Bond angles				
Atoms	A	B	C	D
C1-C2-C3	109.6(2)	109.7(2)	110.3(2)	110.8(2)
C1-C10-C5	109.2(2)	108.6(2)	107.7(2)	107.7(2)
C1-C10-C9	108.7(2)	108.6(2)	109.3(2)	108.0(2)
C1-C10-C19	109.1(2)	109.5(2)	109.5(2)	109.8(2)
C2-C1-C10	114.7(2)	114.3(2)	114.4(2)	113.8(2)
C2-C3-C4	110.1(2)	110.8(2)	110.6(2)	111.8(2)
C2-C3-O3	107.1(2)	106.9(2)	109.6(2)	105.7(2)
C3-C4-C5	111.0(2)	111.5(2)	111.6(2)	111.2(2)
C3-O3-C28	116.5(2)	117.2(2)	117.1(2)	117.3(2)
C4-C5-C6	120.5(2)	120.1(2)	119.7(2)	120.2(2)
C4-C3-O3	109.3(2)	108.7(2)	106.9(2)	111.1(2)
C4-C5-C10	116.4(2)	116.6(2)	117.1(2)	116.5(2)
C5-C6-C7	125.0(2)	124.6(2)	124.5(2)	124.5(2)
C5-C10-C9	109.3(2)	110.1(2)	110.1(2)	111.0(2)
C5-C10-C19	108.3(2)	108.4(2)	108.6(2)	109.0(2)
C6-C5-C10	123.2(2)	123.3(2)	123.3(2)	123.3(2)
C6-C7-C8	112.6(2)	113.3(2)	112.5(2)	112.0(2)
C7-C8-C9	109.3(2)	110.2(2)	110.0(2)	109.6(2)
C7-C8-C14	110.2(2)	110.4(2)	110.4(2)	112.0(2)
C8-C9-C10	112.0(2)	112.8(2)	112.0(2)	111.8(2)
C8-C9-C11	112.5(2)	111.2(2)	112.0(2)	112.8(2)
C8-C14-C13	115.3(2)	115.5(2)	115.2(2)	114.5(2)
C8-C14-C15	117.8(2)	118.0(2)	118.3(2)	119.0(2)
C9-C8-C14	110.2(2)	109.4(2)	110.1(2)	109.1(2)
C9-C10-C19	112.1(2)	111.7(2)	115.5(2)	111.4(2)
C9-C11-C12	113.9(2)	113.7(2)	113.9(2)	113.8(2)
C10-C9-C11	113.6(2)	113.6(2)	113.1(2)	111.9(2)
C11-C12-C13	111.6(2)	111.1(2)	111.8(2)	111.4(2)
C12-C13-C14	106.5(2)	106.4(2)	106.2(2)	106.1(2)
C12-C13-C17	117.6(2)	116.8(2)	116.3(2)	115.2(2)
C12-C13-C18	109.9(2)	110.3(2)	111.4(2)	111.4(2)
C13-C14-C15	103.6(2)	104.2(2)	104.5(2)	104.2(2)

TABLE 3. Continued

C13-C17-C16	102.1(2)	103.1(2)	103.5(2)	103.6(2)
C13-C17-C20	118.6(2)	120.3(2)	119.6(2)	117.8(2)
C14-C13-C17	99.5(1)	100.1(1)	100.0(1)	101.5(1)
C14-C13-C18	112.2(2)	112.7(2)	112.3(2)	111.9(2)
C14-C15-C16	104.5(2)	103.3(2)	103.3(2)	103.6(2)
C15-C16-C17	106.0(2)	107.2(2)	107.2(2)	107.6(2)
C16-C17-C20	115.4(2)	111.8(2)	111.3(2)	113.2(2)
C17-C13-C18	110.8(2)	110.2(2)	110.1(2)	110.3(2)
C17-C20-C21	109.9(2)	112.7(2)	113.0(2)	112.6(2)
C17-C20-C22	112.4(2)	110.1(2)	109.7(2)	111.7(2)
C20-C22-C23	114.8(2)	115.4(2)	116.1(2)	113.6(2)
C21-C20-C22	109.5(2)	110.3(2)	110.2(2)	110.0(2)
C22-C23-C24	112.5(2)	113.5(2)	112.3(2)	115.0(2)
C23-C24-C25	114.3(2)	115.3(2)	116.4(2)	114.1(2)
C24-C25-C26	111.1(2)	111.5(3)	110.7(2)	111.4(2)
C24-C25-C27	111.9(2)	112.4(2)	113.0(3)	112.0(2)
C26-C25-C27	110.7(2)	109.6(3)	110.2(3)	110.4(2)
C28-C29-C30	115.1(2)	118.0(2)	113.7(2)	113.1(2)
C29-C30-C31	112.3(3)	112.4(2)	112.6(2)	112.6(2)
O3-C28-C29	110.2(2)	112.2(2)	111.0(2)	110.8(2)
O3-C28-O28	124.5(2)	124.0(2)	123.3(2)	123.7(2)
O28-C28-C29	125.2(2)	123.8(2)	125.7(2)	125.6(2)

(c) Selected bond torsion angles

In the view down the central bond, a clockwise twist of the back bond from the eclipsed configuration corresponds to a positive torsion angle.

Atoms	A	B	C	D
C4-C5-C6-C7	-178.0	-178.6	-177.4	-176.5
C10-C5-C6-C7	1.5	0.4	2.4	3.8
C14-C13-C17-C20	-174.1	-165.8	-163.4	-161.7
C15-C16-C17-C20	158.9	150.8	148.0	143.2
C13-C17-C20-C21	-82.0	-55.3	-55.4	-58.6
C13-C17-C20-C22	155.8	-178.9	-178.6	177.2
C17-C20-C22-C23	179.3	-166.8	-160.9	-169.3
C21-C20-C22-C23	56.8	68.2	74.2	65.0
C22-C23-C24-C25	176.1	-172.5	-179.5	-172.6
C23-C24-C25-C26	165.1	169.4	-172.4	173.1
C23-C24-C25-C27	-70.6	-67.1	63.4	-62.7
C1-C2-C3-O3	179.1	177.4	175.5	175.8
C2-C3-O3-C28	156.8	148.9	84.3	159.1
C4-C3-O3-C28	-84.0	-91.5	-155.8	-79.4
O3-C28-C29-C30	163.6	23.9	169.9	151.1
O28-C28-C29-C30	-18.7	-157.8	-10.2	-27.9
C28-C29-C30-C31	175.9	177.5	178.8	-178.0

(d) Intermolecular C...C and C...O distances less than 3.8 Å

There are no O...O distances less than 3.8 Å. Molecules involved are designated as A, B, C, or D in parentheses. Superscripts refer to the following symmetry operations with respect to the atomic coordinates in Table 2:

<i>a</i> : $x, y, 1+z$	<i>e</i> : $2-x, 1/2+y, 1-z$
<i>b</i> : $2-x, 1/2+y, 2-z$	<i>f</i> : $1-x, 1/2+y, 1-z$
<i>c</i> : $2-x, 3/2+y, 2-z$	<i>g</i> : $1-x, 3/2+y, 1-z$
<i>d</i> : $2-x, 3/2+y, 1-z$	

C26(A) ... C31(A) ^e	3.76
C25(A) ... O28(D) ^f	3.66
C27(A) ... O3(D) ^f	3.79
C28(A) ... C18(D) ^f	3.64
C31(A) ... C19(D) ^f	3.71
O3(A) ... C18(D) ^f	3.62
O3(A) ... C15(D) ^f	3.62
C6(B) ... C18(C) ^f	3.80
C23(B) ... O28(C) ^f	3.72
O28(B) ... C25(C) ^f	3.68
C12(B) ... O28(D) ^f	3.28
C18(B) ... C2(D) ^f	3.79
C27(B) ... C11(D) ^f	3.71
C19(C) ... O28(C) ^f	3.37

^aValues in successive columns are for the non-hydrogen atoms in molecules A, B, C and D and are uncorrected for the effects of thermal vibration.

TABLE 4. Molecular moments of inertia

	A	B	C	D
Center of mass	21.66 0.88 26.16	6.58 1.51 7.72	11.53 1.63 17.64	17.63 1.00 9.05
I_1	16592 0.2347 0.9719 0.0160	16405 0.1642 -0.9847 -0.0579	16680 -0.5396 -0.8418 -0.0090	16818 0.8473 0.5302 0.0314
I_2	16296 0.9689 -0.2352 0.0769	16045 -0.9789 -0.1555 -0.1329	16416 -0.8297 0.5336 -0.1639	16375 -0.5310 0.8446 0.0686
I_3	781 0.0785 -0.0026 -0.9969	837 0.1219 0.0785 -0.9894	814 0.1427 -0.0810 -0.9864	718 0.0099 -0.0748 0.9971

Moments of inertia (dalton \AA^2) are calculated with respect to the crystal Cartesian axial system a , b , c^* with the origin at the molecular center of mass. Values were obtained for the configuration of C and O atoms with the mass of each C atom augmented by the mass of any covalently bonded H atoms. The maximum principal value I_1 is the moment of inertia about the axis normal to the best plane through the mass-weighted atoms and the minimum value I_3 is the moment about the best mass-weighted line, which we define as the molecular long axis. Direction cosines are given for each molecule oriented so that the interatomic vectors C10 to C19 and C13 to C10 are in directions approximately along the positive sense of the inertial axes I_1 and I_3 , respectively. Direction cosines are with respect to a , b , c^* in vertical order. So also are the coordinates (\AA) for the center of mass with respect to the origin of the crystal unit cell.

From Table 5 it can be seen that the overall libration has maximum m.s. angular displacements L_z ranging from 12.4 deg² in D to 16.7 deg² in A. The axis for L_z makes a small angle with I_3 ranging from 2.7° in D to 9.9° in B, where I_3 is the axis of minimum moment of molecular inertia, that is, the molecular long axis. The other principal values for overall libration (L_x and L_y) are almost zero. The coupling of the internal torsions with the overall libration is strongest for $\langle \phi_j l_3 \rangle$, that is for libration about the axis of minimum molecular inertia. It should be noted that the coupling term $\langle \phi_1 l_3 \rangle$ is positive in sign, indicating that the overall libration about I_3 tends to be in phase with the internal torsion about the C3-O3 bond. In contrast, the $\langle \phi_2 l_3 \rangle$ and $\langle \phi_3 l_3 \rangle$ couplings are negative, indicating that the overall libration about I_3 tends to be out of phase with the internal torsions in the C17 tails.

The bond lengths and angles in Table 3 have not been corrected for the effects of molecular thermal vibrations. These corrections amount to increases in bond lengths up to 0.004 \AA for bonds at the ends of each molecule.

Molecular packing

The four independent molecules chosen for the asymmetric unit (Table 2) are packed together to form a sheet

perpendicular to the crystal b -axis (Fig. 4). The molecules making up this sheet have centers of mass with y -coordinates in a narrow range (0.88 to 1.63 \AA ; Table 4) so that they are coplanar within 0.75 \AA . Because of the crystallographic twofold screw axis along b , the crystal structure consists of a stacking of such sheets with a separation $b/2 = 4.8 \text{\AA}$ and with successive sheets antiparallel to each other (Fig. 5). In the view down the c -axis (Fig. 6), it can be seen that every molecule has six nearest neighbors, but the details of the arrangement are different for the four independent molecules. There are no unusually short intermolecular distances (Table 3(d)).

The molecules within the sheet shown in Fig. 4 have their long axes nearly parallel except that molecule D is antiparallel to the other three. The angles between molecular long axes I_3 , as calculated from the direction cosines in Table 4, are 5.3, 10.5, and 173.2° for $A^{\wedge}B$, $A^{\wedge}C$, and $A^{\wedge}D$; 12.6 and 172.4° for $B^{\wedge}C$ and $B^{\wedge}D$; 167.4° for $C^{\wedge}D$. However, the orientations of these molecules about their long axes are considerably different. The orientation is estimated from the direction cosine of I_1 with respect to the crystal b -axis, which gives the angle between the best plane of each molecule and the plane of the sheet. These angles are 13.6, 167.0, 147.3, and 58.0° for A, B, C, and D, respectively.

TABLE 5. Molecular thermal vibrations

	A	B	C	D
Agreement criteria:				
R _w	0.130	0.127	0.110	0.111
Goodness-of-fit	3.16	2.98	2.59	2.60
Rigid body tensor components:				
T ₁₁	234(19)	153 (7)	148 (7)	216 (7)
T ₂₂	151(10)	193 (6)	184 (6)	179 (6)
T ₃₃	247 (5)	226 (4)	202 (4)	195 (4)
T ₁₂	32(16)	3 (6)	28 (5)	2 (5)
T ₁₃	- 21 (5)	13 (5)	1 (4)	0 (4)
T ₂₃	8 (5)	- 4 (4)	- 2 (4)	- 11 (4)
L ₁₁	0.9 (1)	0.3 (1)	0.8 (1)	0.7 (1)
L ₂₂	0.3 (2)	1.1 (1)	0.9 (1)	0.5 (1)
L ₃₃	16.7(13)	13.6(11)	14.0 (8)	12.4 (9)
L ₁₂	0.4 (1)	0.0 (1)	0.3 (1)	0.2 (1)
L ₁₃	0.6 (4)	1.2 (2)	- 0.9 (2)	- 0.5 (2)
L ₂₃	0.6 (3)	2.0 (2)	1.1 (2)	- 0.3 (2)
S ₁₁	12(16)	2 (6)	- 16 (5)	9 (5)
S ₁₂	- 2 (5)	6 (3)	16 (3)	- 4 (2)
S ₁₃	6 (5)	6 (5)	- 3 (4)	4 (4)
S ₂₁	- 44(10)	8 (3)	- 8 (3)	- 3 (3)
S ₂₂	- 37	17	13	- 4
S ₂₃	- 3 (6)	16 (5)	- 1 (4)	- 3 (4)
S ₃₁	209(26)	- 158(17)	74(16)	71(14)
S ₃₂	- 39(26)	119(18)	- 79(18)	- 29(16)
S ₃₃	25(32)	- 19(20)	3(18)	- 5(19)
Principal values, T and L:				
T _x	230	151	133	216
T _y	138	193	199	173
T _z	265	228	203	201
L _x	1.0	0.2	0.5	0.8
L _y	0.1	0.8	1.1	0.3
L _z	16.7	14.0	14.1	12.4
Internal torsional vibrations:				
<φ ₁ l ₁ >	- 1.5 (5)	2.4 (7)	1.8 (4)	0.0 (3)
<φ ₁ l ₂ >	- 0.3 (5)	1.2 (5)	- 2.8 (4)	- 1.3 (3)
<φ ₁ l ₃ >	13.9(26)	17.1(24)	9.0(17)	5.3(17)
<φ ₂ l ₁ >	2.1(13)	1.6 (3)	1.4 (3)	- 0.6 (3)
<φ ₂ l ₂ >	- 3.6 (8)	- 0.7 (2)	0.0 (2)	- 0.6 (2)
<φ ₂ l ₃ >	- 6.9(19)	- 20.0(15)	- 4.1(13)	- 5.2 (9)
<φ ₃ l ₁ >	0.2(10)		2.0 (4)	
<φ ₃ l ₂ >	1.4 (9)		0.4 (6)	
<φ ₃ l ₃ >	- 18.8(58)		- 39.7(39)	
M.s. angular displacements about the internal torsional axes: ^d				
Axis 1 <λ ² >	11.2	12.5	13.6	10.5
<(λ + φ) ² >	19.6	45.1	29.5	19.7
Axis 2 <λ ² >	16.2	11.9	9.9	9.1
<(λ + φ) ² >	42.7	45.6	15.6	16.8
Axis 3 <λ ² >	12.5		8.7	
<(λ + φ) ² >	47.1		70.6	

Segmented body thermal parameters are given with respect to the Cartesian axial system of the principle moments of inertia for each molecule (I₁, I₂, I₃) and with the origin at the molecular center of mass (see Table 4). Tensor components are given for overall rigid body translation T (Å² × 10⁴), libration L (degr²) and for the coupling between rigid body translational and librational vibrations S (degr Å × 10³). The coupling between internal torsional vibrations φ_i about selected covalent bonds and the overall rigid body librations l_j about the Cartesian axes j = 1, 2, 3 are given as <φ_i l_j> (degr²). For all four molecules the internal torsion φ₁ is for torsional libration about the C3–O3 bond and involves atomic m.s. displacements which are largest for the butanoate group. The torsional libration φ₂ is about the C17–C20 bond and involves primarily the isoprenoid tail. For molecules A and C an additional torsional libration φ₃ was introduced, this being about C24–C25 for A and C23–C24 for C. The coupling between internal torsional libration and rigid body translation t_i was neglected except for φ₁ in molecule A, where the values obtained were <φ₁ t₁> = - 0.42(12), <φ₁ t₂> = - 0.42(18) and <φ₁ t₃> = 0.15(4) degr Å.

^dHere <λ²> is the contribution to the m.s. angular displacement about the torsion axis owing to rigid-body libration and <(λ + φ)²> is the total m.s. displacement about the same axis.

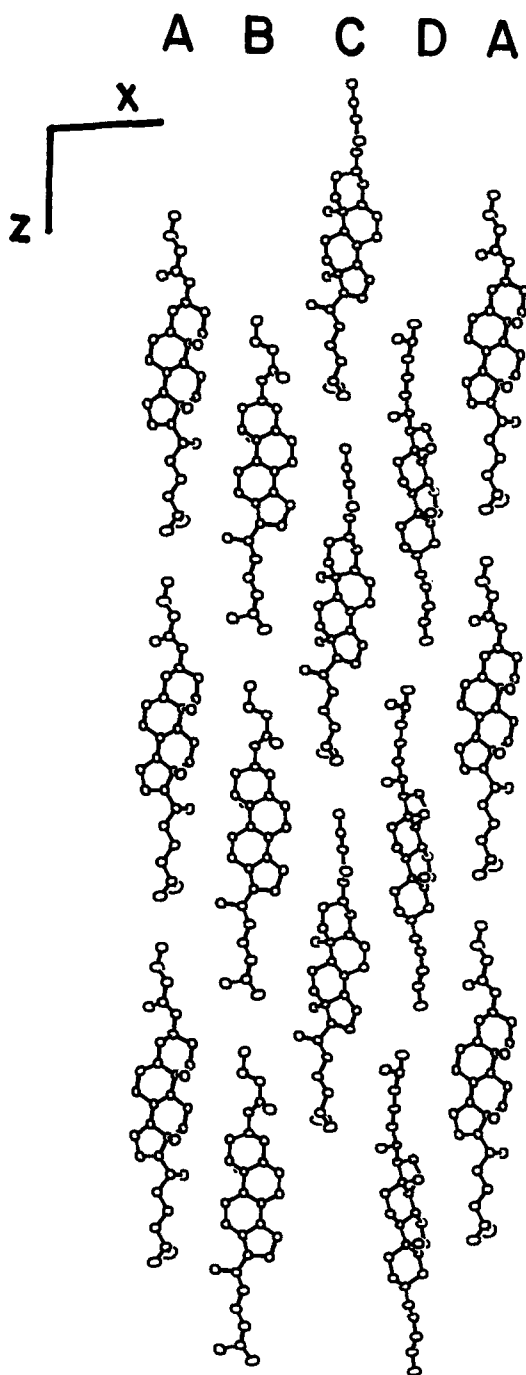


Fig. 4. Molecular packing for an isolated sheet of molecules in the projection down the crystal *b*-axis. Each column, labeled A, B, C, or D, contains three identical molecules related by the unit cell translation *c*. Atoms are represented by 75% probability thermal ellipsoids (21).

As shown in the *b*-projection of the complete crystal structure (Fig. 5), there is extensive overlap of symmetry-related A molecules. This particular stacking arrangement was first observed by Carlisle and Crowfoot (32) in the crystal structure of cholesteryl iodide (polymorph B)

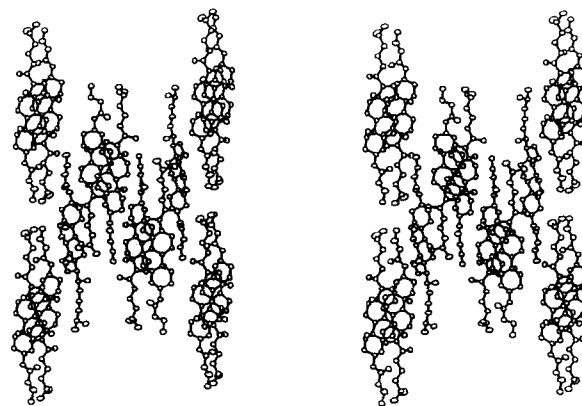


Fig. 5. The complete crystal structure in projection down the *b*-axis. The uppermost layer of molecules corresponds to the sheet shown in Fig. 4. Atoms are represented by 75% probability thermal ellipsoids (21).

and it also occurs in other long chain cholesteryl ester structures which contain monolayers of type II (1). In cholesteryl butanoate, there is additional overlapping (Figs. 5 and 6), but this involves molecules that are unrelated by crystal symmetry. The overlap of molecule B with an antiparallel molecule C in the adjacent sheet is of interest because these molecules are approximately related by local twofold screw axes near $(1/3, y, 1/3)$ and $(2/3, y, 2/3)$. The unusual difficulty in solving the phase problem for this crystal structure may well be attributed to the need for distinguishing this pseudosymmetry from the true crystallographic symmetry.

Structural relationship between the crystalline and cholesteric phases

A powdered sample of cholesteryl butanoate, from which our crystals were grown, was found to transform monotropically to the cholesteric phase at 98°C and then reversibly to an isotropic liquid at 106°C (Table 1(c)). These transformations were observed directly by a polarized light microscope and by differential scanning calorimetry.

As described by de Gennes (33), the cholesteric phase is a twisted nematic mesophase. In a nematic mesophase, the molecules are rod-like and are packed so that near neighbors have their long axes almost aligned. However, there is no short range order in the view down the molecular long axes. This applies to the orientation of molecules about their long axes and to the distribution of the molecular centers of mass. A cholesteric phase involves an assembly of chiral molecules such as the cholesteryl esters. The chirality imposes a tendency for a small twist in the molecular packing and this gives rise to an overall helical structure with a remarkably long repeat, often comparable to the wavelength of visible light.

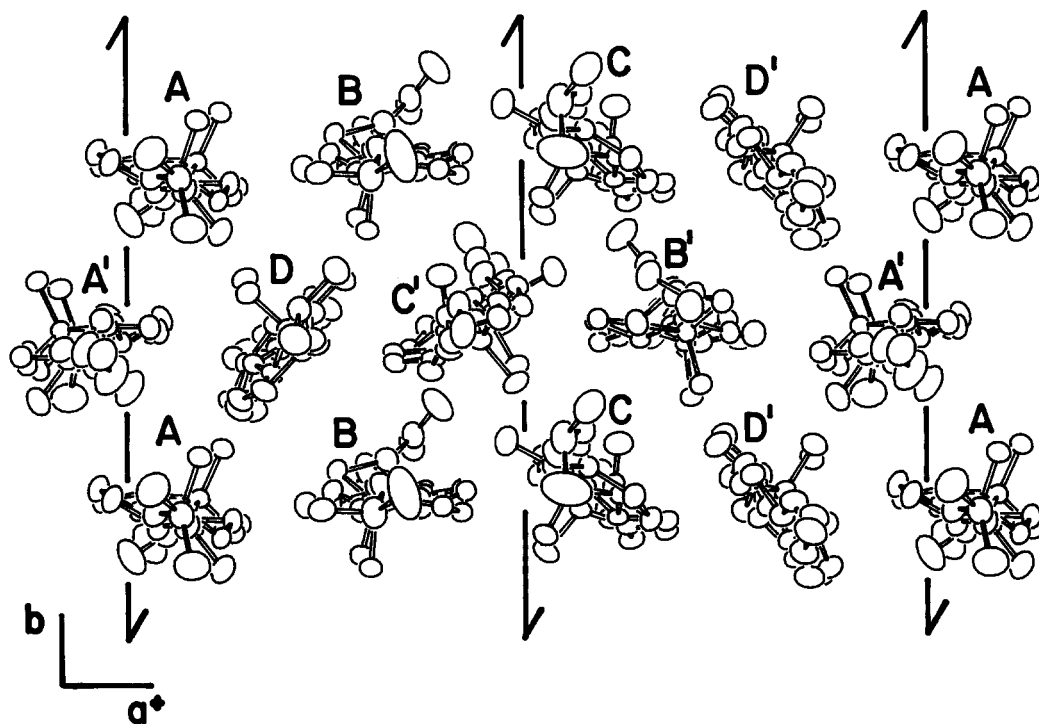



Fig. 6. The crystal structure in projection down the c -axis. The independent molecules are labeled A, B, C, and D. Atom labels with primes are for molecules that are viewed towards the butanoate chain end. The remaining molecules are antiparallel and are viewed towards the cholesteryl tail. The row across the top and bottom are molecules in the sheet shown in Fig. 4. The projecting methyl groups with bonds C13–C18 and C10–C19 almost parallel and superposed are convenient for recognizing the orientation of each molecule about its long axis. Atoms are represented by 75% probability thermal ellipsoids (21).

The crystal structure of cholesteryl butanoate has long range order, but at short range it has some of the characteristics of a nematic mesophase. First, the molecules are rod-like. Although stereochemically the steroid ring system may appear to be lath-shaped, the molecular inertial tensor is very closely represented by an ellipsoid of revolution about the molecular long axis. Thus two of the principal values for the moment of inertia, (I_1 and I_2 in Table 4) differ by less than 3% for all four independent molecules. Second, the molecules have their long axes nearly parallel, the largest angle between the long axes of any pair of molecules being 12.6° . Third, in the three-dimensional packing arrangement, the nearest neighbor arrangement is different for the four independent molecules in the crystal. For example, in Fig. 6 it can be seen that a central molecule A has as its nearest neighbors three that are parallel (one B and two D molecules) and three that are antiparallel (two A and one D molecule), while a central molecule D has four nearest neighbors that are parallel (two A and two B) and two that are antiparallel (one A and one C). Fourth, as shown in Figs. 4 and 6, the four independent molecules have different orientations about their long axes.

In summary, the crystal structure exhibits important characteristics of the liquid crystalline phase, which in fact is obtained when the crystals are heated to 96°C . Cholesteryl butanoate seems well suited for molecular dynamical simulations in order to study this phase transition in further detail. 

We are grateful for the participation of Prof. Yukio Kinoshita in the effort to determine the crystal structure at room temperature. We are also grateful to Prof. William Furey, Jr. and Dr. August Turano for discussions and advice in early stages of this work, and to Dr. John Ruble and Mrs. Joan Klinger for technical assistance. This work was supported by grants HL-20350 and GM-46733 from the National Institutes of Health.

Manuscript received 13 April 1994 and in revised form 14 June 1994.

REFERENCES

1. Craven, B. M. 1986. Cholesterol crystal structures: adducts and esters. *In Handbook of Lipid Research*. 4. D. M. Small, editor. Plenum Press, New York. 149–182.

2. Kang, B. Y., M. J. Chung, and Y. J. Park. 1985. The crystal and molecular structure of cholesteryl formate. *Bull. Korean Chem. Soc.* **6**: 333-337.
3. Chandross, R. J., and J. Bordner. 1978. Cholesteryl chloroformate. *Acta Crystallogr.* **B34**: 2872-2875.
4. Sawzik, P., and B. M. Craven. 1979. The crystal structure of cholesteryl acetate at 123 K. *Acta Crystallogr.* **B35**: 895-901.
5. Weber, H-P., B. M. Craven, P. Sawzik, and R. K. McMullan. 1991. The crystal structure and thermal vibrations of cholesteryl acetate from neutron diffraction at 123 K and 20 K. *Acta Crystallogr.* **B47**: 116-127.
6. Barnard, J. A. W., and J. E. Lydon. 1974. A crystallographic examination of 14 straight chain esters of cholesterol. *Mol. Cryst. Liq. Cryst.* **26**: 285-296.
7. Kim, M. H., Y. J. Park, and C. T. Ahn. 1989. The crystal and molecular structure of cholesteryl isobutyrate. *Bull. Korean Chem. Soc.* **10**: 177-185.
8. Langs, D. A. 1993. Frequency statistical method for evaluating cosine invariants of three-phase relationships. *Acta Crystallogr.* **A49**: 545-557.
9. Gray, G. W. 1956. The mesomorphic behaviour of the fatty esters of cholesterol. *J. Chem. Soc.* 3733-3739.
10. Blessing, R. H. 1987. Data reduction and error analysis for accurate single crystal diffraction intensities. *Crystallogr. Rev.* **1**: 3-55.
11. Craven, B. M. 1975. Computer programs ROTRAN for the determination of crystal structures which contain rigid body fragments of known structure. Technical Report, Department of Crystallography, University of Pittsburgh, USA.
12. Main, P., S. E. Hull, L. Lessinger, G. Germain, J. P. Leclercq, and M. M. Woolfson. 1978. MULTAN, a system of computer programs for the automatic solution of crystal structures from X-ray diffraction data. University of York, England.
13. Yao, J-X. 1981. On the application of phase relationships to complex structures. XVIII. RANTAN—Random MULTAN. *Acta Crystallogr.* **A37**: 642-644.
14. Yao, J-X. 1983. On the application of phase relationships to complex structures. XX. RANTAN for large structures and fragment development. *Acta Crystallogr.* **A39**: 35-37.
15. Woolfson, M. M. 1954. Structure determination by the method of permutation syntheses. *Acta Crystallogr.* **7**: 65-67.
16. Han, G. W. 1993. Crystal structures of lipids. Ph.D. Dissertation, University of Pittsburgh, PA.
17. Langs, D. A., R. Miller, H. A. Hauptman, and G. W. Han. 1994. Use of the minimal function for partial structure development in direct methods. *Acta Crystallogr.* **B50**: submitted.
18. Craven, B. M., H-P. Weber, and X-M. He. 1987. The POP Least Squares Refinement Procedure, Technical Report, Department of Crystallography, University of Pittsburgh, USA.
19. Cromer, D. T., and J. T. Waber. 1965. Scattering factors computed from relativistic Dirac-Slater wave functions. *Acta Crystallogr.* **18**: 104-109.
20. Stewart, R. F., E. R. Davidson, and W. T. Simpson. 1965. Coherent X-ray scattering for the hydrogen atom in the hydrogen molecule. *J. Chem. Phys.* **42**: 3175-3187.
21. Johnson, C. K. 1965. Oak Ridge thermal ellipsoid plot program. Report ORNL-3794. Oak Ridge National Laboratory, Tennessee.
22. Gao, Q., and B. M. Craven. 1986. Conformation of the oleate chairs in crystals of cholesteryl oleate at 123 K. *J. Lipid Res.* **27**: 1214-1221.
23. Nyburg, S. C. 1974. Some uses of a best molecular fit routine. *Acta Crystallogr.* **B30**: 251-253.
24. Cremer, D., and J. A. Pople. 1975. A general definition of ring puckering coordinates. *J. Am. Chem. Soc.* **97**: 1354-1358.
25. Schomaker, V., and K. N. Trueblood. 1968. The rigid-body motion of molecules in crystals. *Acta Crystallogr.* **B24**: 63-76.
26. Hirshfeld, F. L. 1976. Can X-ray data distinguish bonding effects from vibrational smearing? *Acta Crystallogr.* **A32**: 239-244.
27. Rosenfield, R. E., K. N. Trueblood, and J. D. Dunitz. 1978. A test for rigid-body vibrations based on a generalisation of Hirshfeld's "rigid bond" postulate. *Acta Crystallogr.* **A34**: 828-829.
28. He, X-M., and B. M. Craven. 1993. Internal vibrations of a molecule consisting of rigid segments. I. Non-interacting internal vibrations. *Acta Crystallogr.* **A49**: 10-22.
29. Craven, B. M., and X-M. He. 1992. Programs for thermal motion analysis. Technical Report, Department of Crystallography, University of Pittsburgh, PA.
30. Eckart, C. 1935. Some studies concerning rotating axes and polatomic molecules. *Phys. Rev.* **47**: 552-558.
31. Dunitz, J. D., V. Schomaker, and K. N. Trueblood. 1988. Interpretation of atomic displacement parameters from diffraction studies of crystals. *J. Phys. Chem.* **92**: 856-867.
32. Carlisle, C. H., and D. Crowfoot. 1945. The crystal structure of cholesteryl iodide. *Proc. R. Soc., London.* **A184**: 64-83.
33. de Gennes, P. G. 1979. The Physics of Liquid Crystals. Clarendon Press, Oxford. 9.